

## Structural and Optical Properties Studies of Mn<sup>+</sup> Ion Implanted GaAs

SHARAD TRIPATHI<sup>1</sup>, S. K. DUBEY<sup>2</sup>, V. S. UPADHYAY<sup>1</sup>

<sup>1</sup>Department of Physics, G. N. Khalsa College, Matunga, Mumbai, India.

<sup>2</sup>Department of Physics, University of Mumbai, Vidyanagari, Mumbai, India

E- Mail: skdubeymu@gmail.com

### Abstract

*In this study, un-doped GaAs were uniformly implanted with 325 keV Mn<sup>+</sup> ions for the various fluences varying from  $1 \times 10^{15}$  to  $2 \times 10^{16}$  ions cm<sup>-2</sup> using 1.7 MV Tandatron accelerator at IGCAR, Kalpakkam. AFM and UV-Vis-IR techniques were used for their characterization. The AFM image for non-implanted GaAs showed the smooth micrograph relative to the implanted samples and the samples implanted for the fluence of  $1 \times 10^{15}$ ,  $5 \times 10^{15}$ ,  $1 \times 10^{16}$  and  $2 \times 10^{16}$  ions cm<sup>-2</sup> showed the presence of the clusters of different sizes in the range between 52 to 319 nm on the surface of GaAs. The densities of the clusters were found to increase with respect to ion fluences. UV-VIS-NIR spectra of non-implanted and samples implanted for various fluences ranging from  $1 \times 10^{15}$  to  $2 \times 10^{16}$  ions cm<sup>-2</sup> were performed in the spectral region 150 nm to 3300 nm. The values of the absorption coefficient ( $\alpha$ ) of Mn<sup>+</sup> ion implanted GaAs samples estimated from the transmission spectra were found to increase with ion fluence. The increase in absorbance with respect to ion fluence indicates the increase in defects and disorder in the ion implanted layers. The band gap energy of the samples implanted with the fluence of  $1 \times 10^{15}$ ,  $5 \times 10^{15}$ ,  $1 \times 10^{16}$  and  $2 \times 10^{16}$  ions cm<sup>-2</sup> estimated from the  $\alpha^2$  versus photon energy curve were found to be 1.370, 1.332, 1.323 and 1.309 eV respectively.*

**Keywords:** Ion Implantation, GaAs, Mn, AFM, UV.

### Introduction

(GaMn)As is very important dilute magnetic semiconductors because of its potential application in electronics and optoelectronics devices such as blue ultra – violet light emitting diodes and laser diodes, as well as high temperature and high power devices [1-2]. Many methods have been employed to incorporate Mn into GaAs but obstacle occurs to maintain certain percentage of Mn (low solubility limit of magnetic element). Ion implantation is a versatile technique that can produce systems away from the thermodynamic equilibrium. It is a low temperature and cleaner process in which the concentration and depth of the implants can be precisely controlled by proper selection of ion fluence and energy respectively. Excellent uniformity and lateral selectivity can also be achieved by ion implantation. Hence it can be conveniently used to synthesize semiconductor structures that could yield the desired structural, optical and electrical properties. Despite these advantages, ion implantation causes damage in the crystal lattice as ion loses energy during its travel in the crystal. Characterization of damage and its removal by annealing are important to investigate for most of the applications. Some studies on the effects of Mn ion



implantation in GaAs with various fluences at different energies have been reported [3-4]. The 80 keV Mn ions implanted in p-GaAs with fluence of  $7.5 \times 10^{15}$  ions  $\text{cm}^{-2}$  were studied using the Rutherford backscattering spectrometry, particle induced X-ray emission and X-ray absorption techniques were used to investigate the structure [5]. p-type GaAs wafers were implanted with different energies (70, 120, 170, 250 and 350 keV) with various fluences ( $0.9, 0.88, 0.61, 1.3, 0.63 \times 10^{16}$  ions  $\text{cm}^{-2}$ ) at room temperature and after implantation, the samples were irradiated with 350 keV  $\text{He}^+$  ions with fluence of  $1 \times 10^{16}$  ions  $\text{cm}^{-2}$  for Recrystallization [6]. Semi-insulating GaAs implanted with 1 MeV  $\text{Mn}^+$  with fluence of  $3 \times 10^{15}$  ions  $\text{cm}^{-2}$  were studied using the high resolution X-ray diffraction, Fourier transform infrared, Scanning electron microscopic, Raman scattering and vibrating sample magnetometer [7-8].

In the present work, we studied the structural and optical properties of gallium arsenide after implantation with 325 keV  $\text{Mn}^+$  ions with various fluences varying from  $1 \times 10^{15}$  to  $2 \times 10^{16}$  ions  $\text{cm}^{-2}$  using Atomic Force Microscopy and UV-Vis-IR techniques.

### Experiment details

In this study, un-doped gallium arsenide samples were implanted with 325 keV  $\text{Mn}^+$  ions for the fluences of  $1 \times 10^{15}$ ,  $5 \times 10^{15}$ ,  $1 \times 10^{16}$  and  $2 \times 10^{16}$  ions  $\text{cm}^{-2}$  using 1.7 MV Tandem accelerators at IGCAR, Kalpakkam. The implantation energy of 325 keV was selected on the basis of the SRIM code calculations. Projected range ( $R_p$ ) and standard deviation ( $\Delta R_p$ ) of the 325 keV  $\text{Mn}^+$  ions in gallium arsenide were found to be 155.6 nm and 66.7 nm respectively (Fig.1). The beam current density was about  $50 \text{ nA cm}^{-2}$  during implantation. The scanned beam was further collimated through a collimator of diameter 12.5 mm for uniform implantation over the entire area of the sample. During implantation, the vacuum in the target chamber was maintained at  $10^{-7}$  mbar. The morphology of the samples was examined using atomic force microscope (*Nanoscope-III*) with silicon nitride tip. Different areas ( $5 \mu\text{m} \times 5 \mu\text{m}$ ) were scanned in the implanted and non-implanted samples in tapping mode. The scanned AFM images had  $1000 \times 1000$  point resolution. The various parameters such as average roughness, root mean square roughness, peak height, valley depth, surface skewness, surface kurtosis, grain size and its histograms evaluated from the AFM data using the SPIP software version 5.03 and UV-VIS-NIR transmission spectra were performed on UV-VIS-NIR spectrometer (Shimadzu UV-3600) in wavelength regions 150 nm to 3300 nm. This spectrometer is equipped with three detectors; a photomultiplier tube (PMT) for the UV- VIS region, and InGaAs and PbS detectors for the NIR region. The three detectors ensure high sensitivity over the entire measurement range and help to achieve the lowest noise level. A high-performance double monochromator ensures ultra-low stray light at high resolution have been used to investigate optical properties of  $\text{Mn}^+$  ion implanted samples.

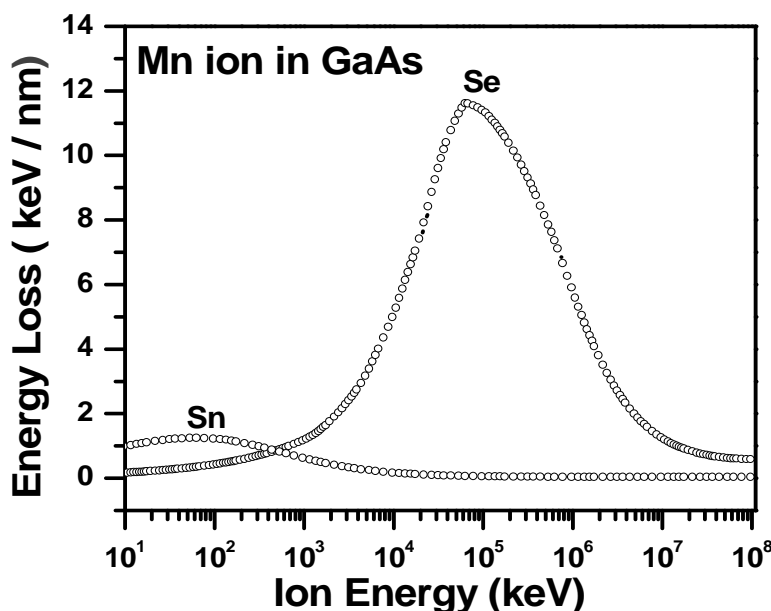


**Figure 1:** Variation of nuclear energy loss and electronic energy loss as a function of ion energy for Mn ions in gallium arsenide.

## Results and Discussion

### Atomic Force Microscopy Study

Three dimensional atomic force microscopy images along with histograms ( $5\mu\text{m} \times 5\mu\text{m}$ ) of samples implanted at fluence of  $1 \times 10^{15}$ ,  $5 \times 10^{15}$ ,  $1 \times 10^{16}$ ,  $2 \times 10^{16}$  ions  $\text{cm}^{-2}$  are shown in Fig. 2(a), 2(b), 2(c), 2(d) respectively. The image obtained from the non-implanted sample showed a smooth micrograph with root mean square surface roughness of 0.49 nm. Three dimensional AFM micrographs of all implanted samples revealed hillock-like features accompanied by trough-like features and the most of the cluster's height in range of 6 - 13 nm (Fig. 2(a, b, c, d)). The compression of the target on impact of energetic manganese ions originates high temperature that leads local melting of target. Excavation of target material at impact spot leads to simple crater formation. Local tensions and elastic rebound push out a melt causing hillock formations [9]. Average roughness, average height, surface skewness, surface kurtosis, r. m. s. roughness and diameter of clusters evaluated from AFM data are given in Table -1. The increase in the roughness with ion fluence indicated the impact of the manganese ions on the surface of GaAs [10]. The positive value of surface skewness showed the predominance of peaks. The surface kurtosis ( $R_{ku}$ ) measure the distribution of spikes above and below the mean line. For spiky surface,  $R_{ku} > 3$  and for bumpy surface  $R_{ku} < 3$ , this implied that the (Table -1) surface of GaAs is spiky.

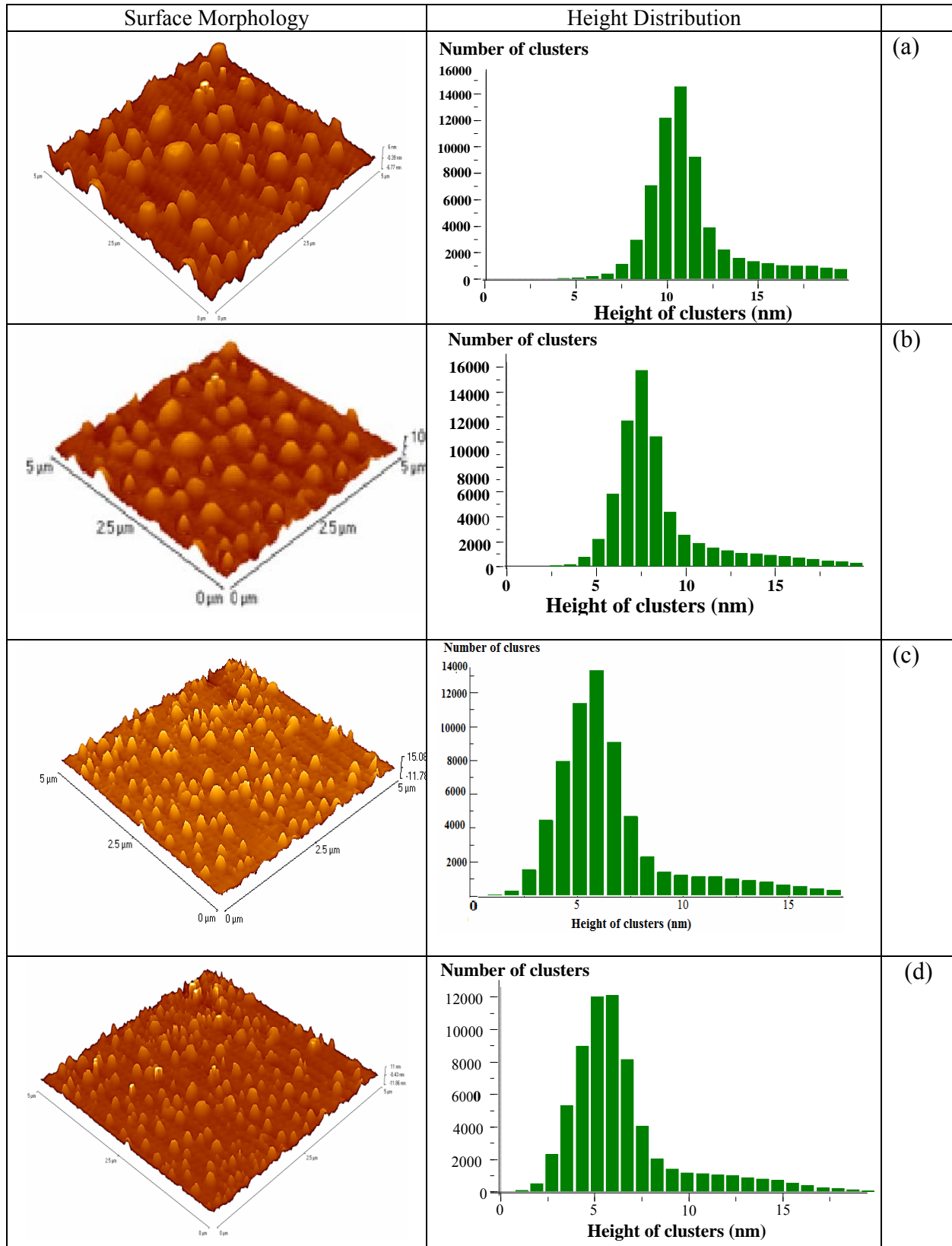


**Figure 2:** Three dimensional AFM images with histograms of GaAs (a) non-implanted and implanted with 325keV Mn ions at fluence of (b)  $1 \times 10^{15}$ , (c)  $5 \times 10^{15}$ , (d)  $1 \times 10^{16}$ , (e)  $2 \times 10^{16}$  ions  $\text{cm}^{-2}$ .

Table 1: Various parameters of clusters evaluated from AFM data.

Ion fluence (ions cm <sup>-2</sup> )	Non-implanted	1 x 10 <sup>15</sup>	5 x 10 <sup>15</sup>	1 x 10 <sup>16</sup>	2 x 10 <sup>16</sup>
Average roughness (nm)	0.18	0.74	1.43	1.71	2.42
Average height (nm)	1.66	2.30	5.60	8.34	9.41
Surface skewness	0.32	0.88	1.19	2.19	3.32
Surface kurtosis	8.91	10.61	18.80	34.82	44.33
r. m. s. roughness(nm)	0.49	1.23	1.89	2.96	3.77

### Ultra-Violet Visible (UV-VIS) NIR Study

UV-VIS-NIR transmission and reflectance spectra were performed on UV-VIS-NIR spectrometer (Shimadzu UV-3600) in wavelength regions 150 to 3300 nm. UV-Vis-NIR studies were performed on non-implanted and the samples implanted for the fluence of 1 x 10<sup>15</sup>, 5 x 10<sup>15</sup>, 1 x 10<sup>16</sup> and 2 x 10<sup>16</sup> ions cm<sup>-2</sup>. Transmission spectra of the samples implanted with 325 keV Mn<sup>+</sup> ions in range fluence between 1 x 10<sup>15</sup> to 2 x 10<sup>16</sup> cm<sup>-2</sup> are shown in Figure 3. The values of transmittance of the Mn<sup>+</sup> ion implanted samples were found to be decreased, while absorbance of these samples was found to be increased with respect to ion fluence. For direct band gap materials like GaAs, momentum conserving transitions between parabolic bands and absorption coefficient increases with the square root of photon energy. In order to estimate the optical band gap  $\alpha^2$  versus photon energy curve were plotted (Fig. 4). The non-implanted GaAs shows a band gap of 1.393 eV while the band gap energy of the samples implanted at the fluence of 1 x 10<sup>15</sup>, 5 x 10<sup>15</sup>, 1 x 10<sup>16</sup> and 2 x 10<sup>16</sup> ions cm<sup>-2</sup> were found to be 1.370, 1.332, 1.323 and 1.309 eV respectively, which clearly shows a shift in band gap. This shift in band gap is possible due to the strain induced in GaAs lattice due to Mn ion incorporation [6].

The optical density ( $\alpha \cdot d$ ) was calculated from the measured spectra by using the following expression taking into account the multiple reflections;

$$\frac{I}{I_0} = \frac{(1-R)^2 e^{-\alpha d}}{1-R^2 e^{-2\alpha d}}$$

where  $I_0$  and  $I$  are incident and transmitted intensities respectively,  $d$  (= 350  $\mu\text{m}$ ) is the thickness of the sample. The reflectivity ( $R$ ) of gallium arsenide was estimated using the following expression;

$$R = \frac{(n-1)^2 + k^2}{(n+1)^2 + k^2},$$

where  $n$  (= 3.3) is the refractive index and  $k = \lambda \alpha / 4\pi$  is the propagation constant. The value of  $R$  determined using the above equation was found to be 0.34 and assumed to be constant over the entire photon energy range. Figure 5 shows the optical density ( $\alpha \cdot d$ ) versus photon energy curves for both non-

implanted and samples implanted for the fluence of  $1 \times 10^{15}$ ,  $5 \times 10^{15}$ ,  $1 \times 10^{16}$  and  $2 \times 10^{16}$  ions  $\text{cm}^{-2}$ . The increase in the optical density with ion fluence (Figure 5) indicates the increase in the defects and disorder in the implanted layer. The defect-densities in the implanted samples were estimated from Figure 3 using the following relation;

$$N_s = \left[ \frac{m_e c \varepsilon}{2\pi \hbar e^2} \right] \left[ \frac{\mu(1-2\mu^2)^2}{18\mu^4 f} \right] \int \alpha(\text{excess}) dE$$

where  $\int \alpha(\text{excess}) dE$  is the difference in the areas of non-implanted and samples implanted with different ion fluence extracted from Figure 5,  $\mu$  is the refractive index,  $c$  is the speed of light,  $e$  is the electronic charge and  $f$  is the oscillator strength and has been assumed to be one. In this calculation, the density of defects in the samples implanted with ion fluences of  $1 \times 10^{15}$ ,  $5 \times 10^{15}$ ,  $1 \times 10^{16}$  and  $2 \times 10^{16}$  ion  $\text{cm}^{-2}$  were found to be  $1.27 \times 10^{16}$ ,  $1.51 \times 10^{16}$ ,  $1.82 \times 10^{16}$  and  $2.38 \times 10^{16}$   $\text{cm}^{-3}$  respectively.

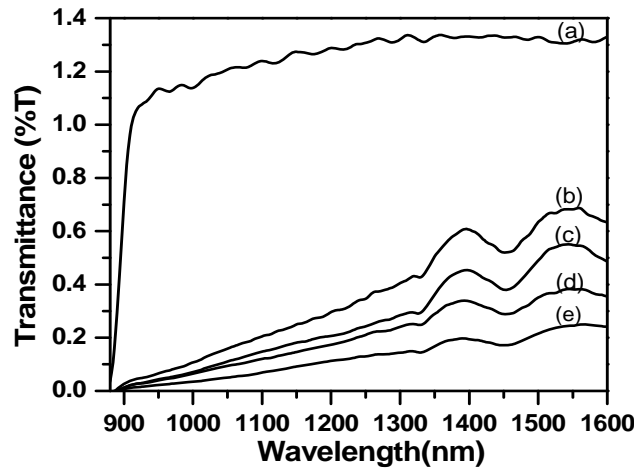


**Figure 3:** Transmission spectra of gallium arsenide; (a) non-implanted and implanted with 325 keV  $\text{Mn}^+$  ions at fluence of (b)  $1 \times 10^{15}$ , (c)  $5 \times 10^{15}$ , (d)  $1 \times 10^{16}$  and (e)  $2 \times 10^{16}$  ions  $\text{cm}^{-2}$ .

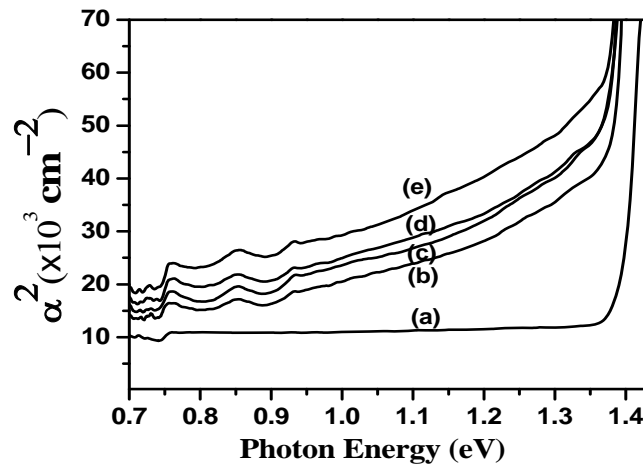


**Figure 4:**  $\alpha^2$  versus photon energy spectra of gallium arsenide; (a) non-implanted and implanted with 325 keV  $\text{Mn}^+$  ions at fluence of (b)  $1 \times 10^{15}$ , (c)  $5 \times 10^{15}$ , (d)  $1 \times 10^{16}$  and (e)  $2 \times 10^{16}$  ions  $\text{cm}^{-2}$ .

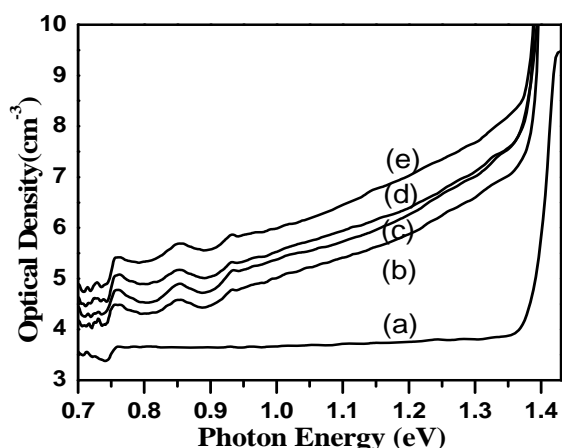


**Figure 5:** Optical density vs photon energy curves of GaAs; (a) non-implanted and samples implanted with 325 keV  $Mn^+$  ions at fluence of (b)  $1 \times 10^{15}$ , (c)  $5 \times 10^{15}$ , (d)  $1 \times 10^{16}$  and (e)  $2 \times 10^{16}$  ions  $cm^{-2}$ .

## Conclusions

The 325 keV  $Mn^+$  ion implantation in semi-insulating GaAs was carried out with various fluences. Three dimensional AFM micrographs of all implanted samples revealed hillock-like features accompanied by trough-like features on the surface of GaAs. The density of the clusters, size of the clusters, r.m.s. roughness the peak height, valley depth, surface skewness, surface kurtosis estimated from the AFM data were found to be depend on the ion fluence. UV-Vis-NIR studies revealed the increase in the absorption with increase in ion fluence.

## Acknowledgments

The authors are thankful to G. N. Khalsa College, Matunga, Mumbai and Maharashtra for providing the financial support and others.

## References

1. H. Ohno, Science 281(1998) 951.
2. Ying Shi, Yong-xing Zhang, Physica B 388 (2007) 82.
3. K.Y.Wang, K.W. Edmonds, R.P. Campion et al, J. Appl. Phys. 95, (2004) 6512
4. Anupama Chanda, H. P. Lenka, Chacko Jacob, Appl Phys A (2009)94:89-94
5. M. Bolduc, C. Awo-Affouda, A. Stollenwerk, Phys. Rev. B 71, (2005) 033302
6. S. Tripathi, R. L. Dubey, S. K. Dubey, A. D. Yadav, P. Kumar and D. Kanjilal, American Institute of Physics 1313 (2010) 100.
7. F. Matsukura, A. Oiwa, A. Shen, Y., J. Cryst. Growth 175/176, (1997). 1069
8. E. De Biasi, M. A. A. Pudenzi, M. Knobel, journal of Magnetic Materials 320 (2008) 404 -407.
9. S. Tripathi, S. K. Dubey, A. D. Yadav, D. C. Kothari et al, DAE SS P Symposium 54 (2009)1064.
10. S. Tripathi, S. K. Dubey, A. D. Yadav and D. C. Kothari, B. K. Panigrahi and K. G. M. Nair,
11. American Institute of Physics 1276 (2009) 344